Physico-chemical Properties of Semi-Organic (Hexakis) Thiocarbamide Nickel(II) Nitrate Single Crystal

V. Revathi[a]*, K. Karthik[b]
[a]Department of Physics, Jaya College of Arts and Science, Thiruninravur, Chennai-602024, Tamil Nadu, India
[b]School of Physics, Bharathidasan University, Tiruchirappalli 620 024, Tamil Nadu, India

Abstract - This work investigates the various properties of (Hexakis) Thiocarbamide Nickel(II) Nitrate (HTNN) single crystal grown by solvent evaporation of mixed ethanol and deionized water at room temperature. The cell parameters and the crystalline nature of the grown crystal were revealed by X-ray diffraction studies. The grown crystal was subjected to FTIR and UV-vis-NIR studies to identify its various functional groups and optical behaviour. The dielectric studies for different frequencies and temperature were performed to the as grown crystal. The melting point and different stage of decomposition of the grown crystal was confirmed by the thermal analysis. The growth mechanism and mechanical strength of the crystal was studied using etching and microhardness measurement.

Keywords: Solvent Evaporation Method; Semi-Organic Crystal; Thiocarbamide; Microhardness and Dielectric Studies.

I. Introduction

Metal-organic compounds have attracted much more attention for their stable physic-chemical properties and better mechanical intension. The Thiocarbamide molecule is an interesting inorganic matrix modifier due to its large dipole moment [1] and its ability to form an extensive network of hydrogen bonds [2]. The metal complexes of Thiocarbamide which have lower UV cut off wavelengths, applicable for high power frequency conversion have received much attention. Ligands like Thiocarbamide form stable complexes through coordinated bonds by S and N donors, which are adequate to combine with metal [3]. The centrosymmetric Thiocarbamide molecule, when combined with inorganic salt yields noncentrosymmetric complexes, which have the NLO properties [4] and also some of them found centrosymmetric in nature [5-7].

In this present work, as grown (Hexakis) Thiocarbamide nickel nitrate crystal is investigated and their structural, optical, electrical and mechanical properties of the crystal are also evaluated.

II. Experimental

Synthesis and Crystal Growth

AR grade materials were used for the synthesis of (Hexakis) Thiocarbamide Nickel(II) Nitrate (HTNN) crystal by solvent evaporation technique. Thiocarbamide and nickel nitrate were taken in 6:1 molar ratio and dissolved in a mixed solvent of ethanol and de-ionized water (1:1 ratio) under constant stirring for 1h. Thus obtained solution was filtered to remove the insoluble impurities and allowed to evaporate at room temperature. Optically good quality crystals of size $13\times13\times3cm^3$ were harvested in a time span of 30 days. The chemical reaction involved in the formation of the as grown crystal is given in Eqn 1. The photograph of the as grown HTNN crystal is shown in Fig. 1. The purity of the crystals was increased by the repeated recrystallization process.

$$6[CS(NH_2)_2] + Ni(NO_3)_2.6H_2O \rightarrow [Ni[CS(NH_2)_2]_6](NO_3)_2 \quad (1)$$

Thiocarbamide Nickel nitrate HTNN

Fig. 1 As grown crystal of HTNN

Characterization

Single crystal X-Ray Diffraction (SXRD) studies were carried out by using the BRUKER axs diffractometer with MoK_α radiation (λ=0.71069Å). The reflection planes of the grown crystals were identified by the Powder X-Ray Diffraction pattern (PXRD) of the powdered sample by using PHILIPS 'X'Pert Pro Radiation CuKα X-ray diffractometer. The molecular structure was confirmed by the FTIR (SHIMADZU-8400S) Spectrophotometer. The optical spectra were recorded by using the Lambda 35 UV-vis-NIR spectrophotometer in the range from 200 to 1100 nm. The dielectric properties were characterized by the HIOKI 3532-50 LCR HITESTER. The mechanical properties were carried out using the Shimadzu HMV-2 Vicker's indentation tester.

III. Results and Discussion

X-ray Diffraction Analysis

Single crystal X-ray diffraction analysis of the grown HTNN crystal was carried out to determine the crystal system and space group. The crystal belongs to monoclinic system with the space group of C2/c. The obtained lattice parameter values are given in Table 1 and they agree well with the reported values [8-11]. The powder X-ray diffraction pattern of the as grown HTNN crystal was recorded in the range of 10-70° using CuKα radiation with a scan speed of 1°/min as shown in Fig. 2. The sharp and intense peaks in the pattern confirm the high crystallanity and good quality of the crystal [12]. Further the 2θ values were taken as the input data for the calculation of (h k l) indices of the reflected planes using Powder X software. Moreover, d values and hkl values of the LPCC crystal are given in Table 2.

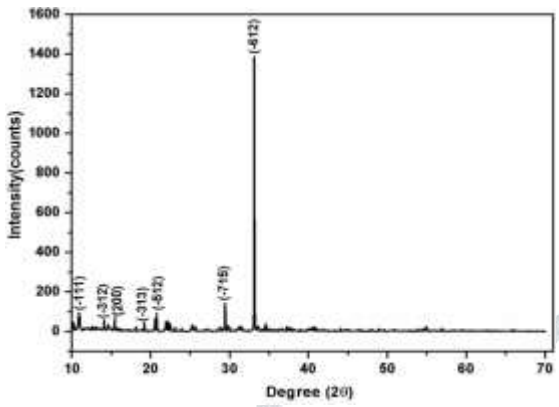

Fig. 2 Powder XRD pattern of HTNN

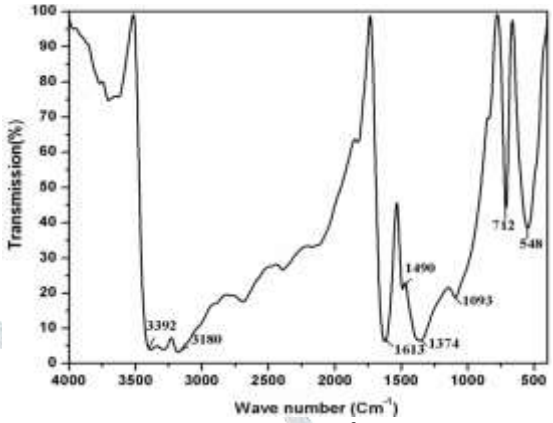

Fig. 3 FTIR spectrum of HTNN

Table 1 & 2 Crystallographic and Indexed X-ray powder diffraction data of HTNN

Crystal data	HTNN
Crystal System	Monoclinic
Space group	C2/c
a(Å)	22.33
b(Å)	9.19
c(Å)	17.29
β(degree)	133.79
Volume($Å^3$)	2652
Crystal colour	Green

h	k	l	d cal.(Å)	2θ cal.(°)
-1	1	1	10.880	8.12492
-3	1	2	6.29679	14.053
2	0	0	5.81344	15.229
-3	1	3	4.56975	19.409
-5	1	2	4.27414	20.766
-7	1	5	3.03887	29.367
-6	1	2	2.70210	33.127

FTIR Spectral Analysis

Fourier transform infrared spectra of HTNN crystal was carried out between 4000 and 400 cm^{-1} as shown in Fig. 4. The broadband between 2750 and 3500 cm^{-1} in the spectrum indicates symmetric and asymmetric stretching modes of NH_2 group of Thiocarbamide and a peak at 1613 cm^{-1} corresponding to NH_2 bending [13]. The peak observed at 1093 cm^{-1} is attributed to the NH_2 rocking [14]. The N-C-N stretching vibration is observed in the spectrum at 1490 cm^{-1} [13]. The peak observed at 548 cm^{-1} represents the N-C-N bending vibration [15]. Further the peaks observed at 1374 and 712 cm^{-1} in the spectrum are due to asymmetric and symmetric stretching of C=S vibration [16].The result confirms the formation of the HTNN crystal and the obtained vibrational frequencies are well matched with the reported values [11].

UV-vis-NIR Studies

UV-vis-NIR spectrum of HTNN crystal was recorded in the range of 200-1100 nm with a scanning speed of 400 nm/min. The absorption spectrum of the as grown crystal of HTNN is depicted in Fig. 4 with cut off wavelength at 415 nm. The HTNN crystal has very minimum absorption in the range between 500-600nm and 850-950 nm.

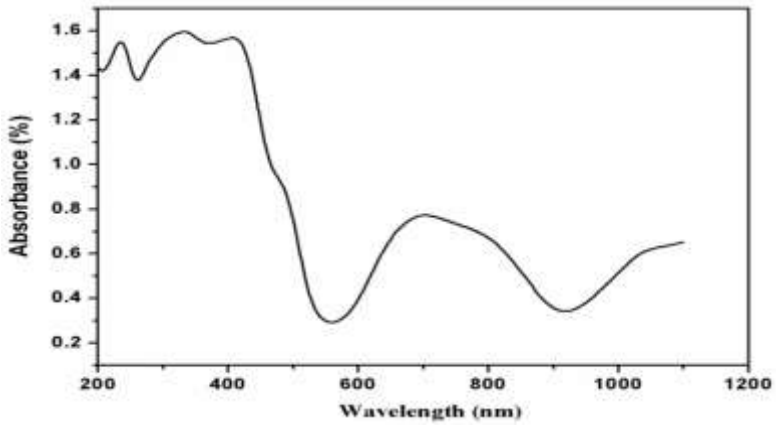

Fig. 4 UV-vis-NIR spectrum of HTNN

Dielectric Studies

The dielectric characteristics of the material give the information about the nature of atoms, ions, bonding and their polarization mechanism in the material. The sample of dimension 9.54×6.66×3.41mm^3 was coated with silver on the opposite faces and placed between the two copper electrodes, to form parallel plate capacitors. The experiment was carried out in the frequency range between 500Hz-5MHz for different temperatures (313,323 and 333K) in order to find the capacitance of the sample. Further the dielectric constant and dielectric loss of the grown crystal were calculated using Eqns 2 and 3 as shown in Fig. 5 respectively.

$$\varepsilon_r = \frac{C_p t}{\varepsilon_0 A} \quad (2)$$

$$\tan\delta = \varepsilon_0 D \quad (3)$$

where C_p is the parallel plate capacitance of the sample in Farad, t is the thickness of the sample in meter, ε_o is the permittivity of free space (8.854×10^{-12} F/m), A is the area of cross section of the sample in m^2, tan δ is the tangent loss and D is the dissipation factor.

It is noted from the Fig. 5a that the dielectric constant decreases exponentially with increasing frequency at different temperatures. The value of dielectric constant is high at low frequency because of the presence of all the four polarizations but not at high frequency due to the presence of only space-charge polarization. It is further noted that at lower frequencies dielectric constant changes more with respect to temperature as compared to higher frequencies which remains constant. It may be due to space charge polarization which is generally active at lower frequencies and high temperatures [17]. Some peaks (Fig. 5) are observed may be due to the resonance effects on electro-optic coefficients, at certain frequencies. The reason for this may be that standing waves are established in the crystal through the inverse piezoelectric effect for certain critical frequencies of the applied field and these critical frequencies are dependent on the dimensions of the crystal studied [18]. The resonance of these stationary waves with the applied electric field at selected frequencies leads to the observed peaks [19]. It is evident from the Fig. 5 that the value of dielectric loss is also decreases with increasing frequency. The characteristic of low dielectric loss at high frequencies clarifies that the grown crystal possesses enhanced optical quality with lesser defects [20].

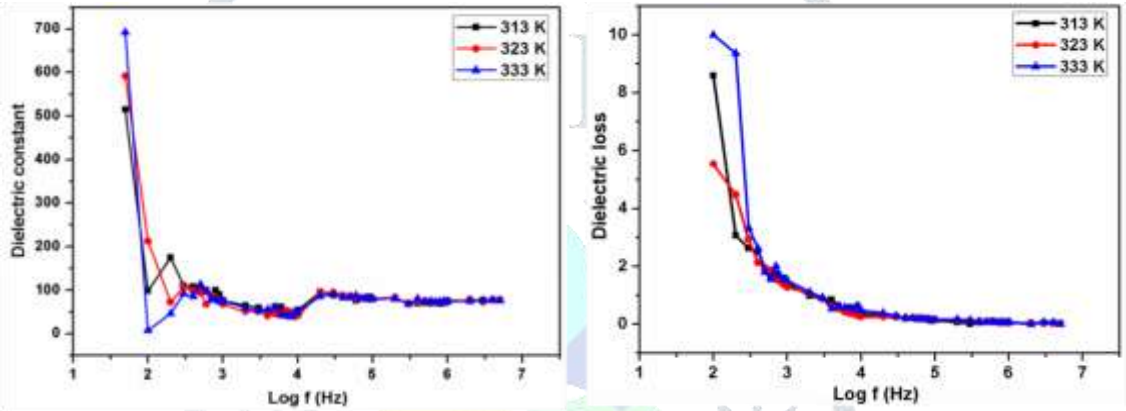

Fig. 5 Dielectric constant and loss of HTNN

Mechanical Studies

Microhardness testing is performed on the as grown crystals to evaluate the mechanical properties by measuring the resistance of the lattice against the applied load. The Vickers hardness number of the materials Hv is determined by the relation,

$$H_v = 1.854\,\frac{P}{d^2}\ (Kg/mm^2) \quad (4)$$

where H_v is the Vickers microhardness number, P is the applied load and d is the average diagonal length of the indentation impression. 1.854 is a constant of a geometrical fraction for the diamond pyramidal indenter.

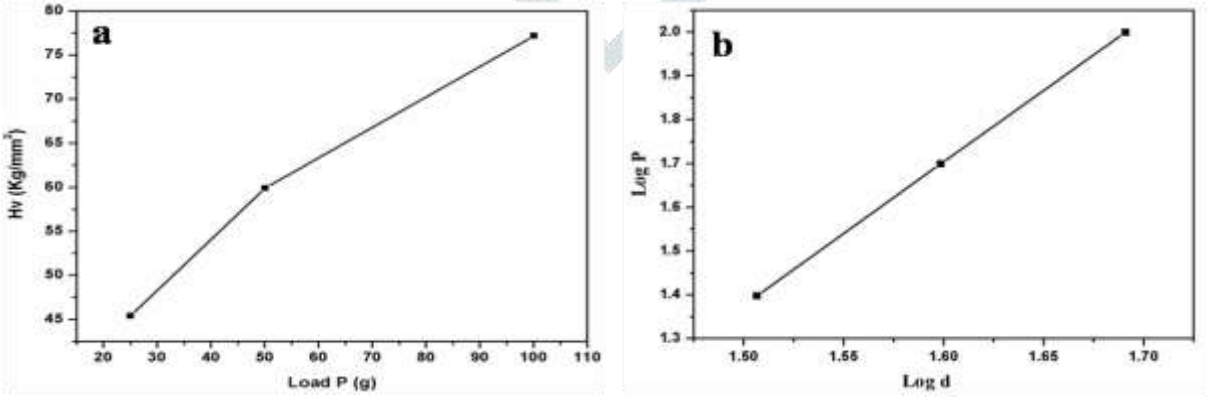

Fig. 6 (a) Load (P) vs H_v and (b) Log P vs Log d

A graph was plotted between hardness number (H_v) and applied load P as shown in Fig. 6a. It is found that the hardness value increases with the increasing of load which exhibits the Reverse Indentation Size Effect (RISE). The load variation can be interpreted by using Meyer's law (Meyer 1908):

$$P = K_1 d^n \quad (5)$$

$$\text{Log } P = \text{Log } K_1 + n \text{ Log } d \quad (6)$$

where K_1 is the material constant and n is Meyer's index. The 'n' value was determined using Eqn 6 by least square fitting method from the graph of Log P versus Log d as shown in Fig. 12 and it is found to be 3.27. According to Onitsch [21] the value of 'n' is less than 1.6 for

hard materials and more than 2 for soft ones. Hence it is concluded that HTNN crystal belongs to soft material category. Hays and Kendall's [22] theory of resistance pressure, explains a relationship between indentation test load (P) and indentation size (d) by assuming the following Eqn:

$$P - W = Kd^2 \quad (7)$$

Substituting the expression of Eqn 5 for P in Eqn 7, we have

$$d^n = (K_2/K_1)\, d^2 + (W/K_1) \quad (8)$$

where W is the sample resistance pressure and represents the minimum load that causes an indentation, K_1 and K_2 are constant. The yield strength of the material can be calculated using the formula [23],

For n>2
$$\sigma_v = \frac{H_v}{2.9}[1-(n-2)]\left[\frac{12.5(n-2)}{1-(n-2)}\right]^{(n-2)} \quad (9)$$

which is a measure of minimum stress required to resist permanent deformation. The elastic stiffness constant (C_{11}) were calculated using the hardness number with Wooster's empirical relation [24],

$$C_{11} = (H_v)^{7/4} \quad (10)$$

which gives an idea about the tightness of bonding between the neighbouring atoms. The hardness parameter values were calculated using Eqn 9 by least square fitting of the plot d^n versus d^2 as shown in Fig. 7 and are given in Table 4. The calculated yield strength (σ_v) and stiffness constant (C_{11}) of the HTNN crystal [25] are tabulated in 5 respectively indicates the strong binding forces between the ions. The higher value of mechanical strength of HTNN crystal confirms its application for the fabrication of devices.

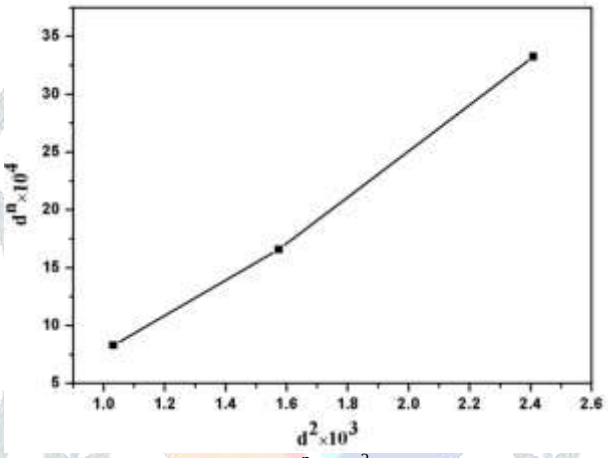

Fig. 7 Plot of d^n vs d^2 of HTNN

Table 4 & 5: The hardness parameters and Mechanical properties of HTNN

Parameters	HTNN
'n'	3.27
K_1 (Kg/m)	3.0097×10^2
K_2 (Kg/m)	5.4925×10^5
W (g)	2.4053×10^{-3}

Load P(g)	C_{11} (GPa)	σ_v (GPa)
25	0.7803	0.7272
50	1.2616	0.9570
100	1.9992	1.2450

4. Conclusion

The monoclinic structure of single crystal of (hexakis) Thiocarbamide nickel(II) nitrate was grown by slow evaporation technique. The monoclinic system and crystalline nature of HTNN was revealed by X-ray diffraction studies. Optical absorption studies show that very minimum absorption in the range between 500-600 nm and 850-950 nm. Microhardness studies reveal the soft material category of the crystal. The calculated yield strength (σ_v) and elastic stiffness constant (C_{11}) indicates the tightness of the bonding between the neighbouring atoms for the grown crystal.

IV. References

[1] K.H. Hellwege, A.M. Hellwege, Landolt–Bornstein: Numerical Data and Functional Relationships in Science and Technology Group II, Springer, Berlin, 1982.
[2] S.G. Bhat, S.M. Dharmaprakah, *Mater. Res. Bull.* 33, 833, 1998.
[3] N. Karthick, R. Sankar , R. Jayavel , S. Pandi, *J. Cryst. Growth.* 312, 114, 2009.
[4] S. Anie Roshan, Cyriac Joseph, M.A. Ittyachen, *Mater. Lett.* 49, 299, 2001.
[5] G. Senthil Murugan, P. Ramasamy, *J. Cryst. Growth* 311, 585, 2009.
[6] M. Lydia Caroline, S. Vasudevan, *Mater.Chem.Phys.* 113, 670, 2009.
[7] G. Senthil Murugan, N. Balamurugan, P. Ramasamy, *Mater. Lett.* 62, 3087, 2008.
[8] J. Madar, *Acta Crystallographica*. 14, 894, 1961.
[9] M.P. Rodriguez, M. Cubero, R. Vega, A. Morente, J.L. Vazquez, *Acta Crystal- lographica* 14, 1961, 1101.
[10] M.M.U. Mehboob, M. Akkurt, I.U. Khan, S. Sharif, I. Asif, S. Ahmad, *Acta Crystallographica E* 66, 57, 2011.
[11] K. Muthu, S.P. Meenakashisundaram, *J. Cryst. Growth* 352, 158, 2012.
[12] K. Parasuraman, K. SakthiMurugesan, R. Uthrakumar, S. JeromeDas, B. MiltonBoaz, *Physica B* 406, 3856, 2011.
[13] R. Rajasekaran, P.M. Ushasree, R. Jayavel, P. Ramasamy, *J. Cryst. Growth* 229, 563, 2001.
[14] K. Kirubavathi, K. Selvaraju, S. Kumararaman, *Spectrochimica Acta Part A* 71,1, 2001.
[15] G. Pabitha, R. Dhanasekaran, *J. Cryst. Growth*, 362, 259, 2013.

[16] P. A. Angeli Mary, S. Dhanuskodi, *Cryst. Res. Technol.* 36(11), 1231, 2001.
[17] Rajesh P, Ramasamy P. *J. Cryst. Growth* 311, 349, 2009.
[18] S.A. Martin Britto Dhas, G. Bhagavannarayana, S. Natarajan, *J. Cryst. Growth* 310, 3535, 2008.
[19] K. Karthik, S. Dhanuskodi, S. Prabukumar, C. Gobinath, S. Sivaramakrishnan, *J. Mater. Sci: Mater. Electron.* 28, 16509, 2017.
[20] C. Balarew and R. Duhlev, *J.Solid State Chem.* 55, 1, 1984.
[21] E.M. Onitsch, Systematic metallographic and mineralogic structures, *Mikroscopia* 2, 131, 1947.
[22] C. Hays, E.G. Kendall, An analysis of Knoop microhardness, *Metallurgy* 6, 275, 1973.
[23] J.R. Cahoon, W.H. Broughton, A.R. Kutzak, *Metall. Trans.* 2, 1979, 1971.
[24] W.A. Wooster, *Rep. Prog. Phys.* 16, 62, 1953.
[25] V. Revathi, V. Rajendran, *Karbala Int. J. Mod. Sci.* 2, 169, 2016.